



M Ű E G Y E T E M 1 7 8 2

Budapest University of Technology and Economics

*Faculty of Civil Engineering*

*Department of Engineering Geology and Geotechnics*

**Ph. D. Thesis Booklet**

***Theoretical and experimental investigation of the rock  
fracture mechanics, focusing on the failure criteria on the  
intact rock***

PhD candidate

**Samad Narimani Ghourtlar**

Supervisor:

**Dr. Balázs Vásárhelyi**

Budapest, March 2026

## Contents

1. INTRODUCTION.....	3
2. OBJECTIVES.....	5
3. MATERIALS AND METHODS .....	7
4. NEW SCIENTIFIC RESULTS(NSR).....	8
4.1. NEW SCIENTIFIC RESULT (1) .....	8
4.2. NEW SCIENTIFIC RESULT (2) .....	11
4.3. NEW SCIENTIFIC RESULT (3) .....	13
4.4. NEW SCIENTIFIC RESULT (4) .....	16
4.5. NEW SCIENTIFIC RESULT (5) .....	21
5. LIST OF PUBLICATIONS (2017-2023).....	23
6. REFERENCES.....	25

# 1. INTRODUCTION

Experimental observations from uniaxial and triaxial compression tests demonstrate that intact rocks do not behave as perfectly elastic–brittle materials. Instead, their stress–strain response evolves through distinct deformation stages, including crack closure, linear elasticity, crack initiation ( $\sigma_{ci}$ ), crack damage ( $\sigma_{cd}$ ), peak strength ( $\sigma_c$ ), and post-peak softening (Martin & Chandler, 1994; Cai et al., 2004). Among these stages, crack initiation and crack damage thresholds represent critical transition points that control stiffness degradation, strength mobilization, and the onset of unstable fracture propagation. Despite their importance, reliable and consistent identification of these thresholds remains challenging, particularly when different strain-based and acoustic emission techniques yield partially divergent interpretations (Nicksiar & Martin, 2012; Diederichs, 2003).

A further limitation of conventional approaches lies in the treatment of elastic parameters. Young’s modulus ( $E$ ) and Poisson’s ratio ( $\nu$ ) are traditionally considered constant within the elastic range. However, increasing experimental evidence indicates that both parameters exhibit stress dependency, especially in heterogeneous and microcracked rocks (Walsh, 1965; Vásárhelyi & Kovács, 2004; Gercek, 2007). In particular, Poisson’s ratio has been shown to evolve significantly as axial stress approaches crack initiation and crack damage thresholds, reflecting accelerated lateral strain and microstructural degradation (Fan et al., 2018; Yu et al., 2019). Recent investigations on granitic rocks further confirm nonlinear variations of stiffness parameters throughout the loading process (Narimani et al., 2023b; Narimani et al., 2025d; Narimani & Vásárhelyi, 2026a). Ignoring this stress-dependent evolution may lead to inaccurate deformation modeling and misestimation of crack thresholds.

Beyond peak strength, residual strength behavior under confinement represents another critical yet insufficiently quantified aspect of intact rock mechanics. Triaxial testing reveals that residual strength is strongly influenced by confining pressure and damage evolution (Hobbs, 1966; Jaeger, 1969; Kovári & Tisa, 1975). As confinement increases, brittle failure progressively transitions toward ductile behavior, accompanied by nonlinear changes in strength parameters (Cai et al., 2007; Peng & Cai, 2019). More recent studies emphasize that the increase in residual strength with confining pressure may exceed the corresponding increase in peak strength, underscoring the importance of post-peak characterization in deep underground applications (Gao & Kang, 2017; Zhao et al., 2023). However, existing residual strength models, including GSI-based and cohesion-loss approaches, do not consistently capture the coupled effects of confinement and progressive microcrack coalescence.

In parallel with experimental and theoretical developments, data-driven techniques have gained increasing attention in rock mechanics. Machine learning (ML) models, including artificial neural networks (ANN), adaptive neuro-fuzzy inference systems (ANFIS), and hybrid evolutionary algorithms, have been successfully applied to estimate key mechanical properties such as uniaxial compressive strength (UCS) and Young’s modulus ( $E$ ) (Sonmez et al., 2006; Armaghani et al., 2016a; Khatti & Grover, 2023). Recent studies also demonstrate the potential of optimized ANN and hybrid GA/PSO approaches for predicting crack stress thresholds with improved accuracy (Narimani & Vásárhelyi, 2025; Narimani & Vásárhelyi, 2026b). Nevertheless, many of these models remain predominantly empirical and require stronger integration with physically meaningful fracture mechanics parameters.

These limitations collectively reveal a significant scientific gap: current rock fracture mechanics frameworks do not fully integrate stress-dependent elastic behavior, progressive crack evolution, confinement-controlled residual strength, and advanced predictive modeling within a unified methodology. In particular:

- The stress dependency of Poisson’s ratio and stiffness degradation is not systematically incorporated into failure modeling.
- Crack initiation and crack damage thresholds lack standardized, physically robust identification procedures.
- Residual strength evolution under varying confining pressures is not comprehensively linked to brittle–ductile transition mechanisms.
- The synergy between experimental fracture mechanics and optimized machine learning techniques remains underdeveloped.

Motivated by these unresolved challenges, the present doctoral research develops an integrated experimental–analytical–data-driven framework to investigate the failure behavior of intact rocks. The study combines controlled laboratory testing, strain-based analytical interpretation, residual strength modeling, and hybrid machine learning optimization to systematically examine stress-dependent deformation, crack stress thresholds, and post-peak behavior.

The experimental investigations focus primarily on granitic rocks from the Bábaapáti in Hungary, a site of strategic importance for underground engineering applications. The brittle nature and high strength of these rocks make them particularly suitable for investigating crack evolution, stiffness degradation, and confinement-controlled residual behavior (Narimani et al., 2025a; Narimani & Vásárhelyi, 2025).

By bridging classical fracture mechanics concepts with modern predictive modeling techniques, this thesis advances the understanding of intact rock failure beyond peak strength description, emphasizing progressive damage evolution and stress-dependent material behavior. The findings contribute to refining failure criteria, improving deformation modeling, and enhancing predictive reliability in geotechnical engineering practice.

## 2. OBJECTIVES

The general objective of this doctoral research is to develop an integrated experimental–analytical–data-driven framework for describing the stress-dependent failure behavior of intact rocks, with particular emphasis on crack stress thresholds, stiffness evolution, and residual strength under confinement.

This objective is motivated by the recognized limitations of conventional failure criteria and elastic modeling approaches, which primarily describe peak strength while inadequately addressing progressive damage evolution and post-peak behavior (Hoek & Brown, 1997; Labuz & Zang, 2012; Cai et al., 2007).

## 2.1 Specific Objectives

To achieve the general aim, the following specific objectives were defined:

### Objective 1

**To investigate the stress-dependent evolution of elastic parameters, particularly Poisson's ratio, during uniaxial compression of intact rocks.**

Although Young's modulus, Shear modulus, Bulk modulus and Poisson's ratio are commonly treated as constants within the elastic range, experimental evidence demonstrates nonlinear stiffness evolution as microcracking develops (Walsh, 1965; Vásárhelyi & Kovács, 2004; Gercek, 2007). However, systematic formulations describing stress-dependent Poisson's ratio in brittle granites remain limited. This objective aims to quantify this evolution and develop a mathematical description applicable to deformation modelling.

### Objective 2

**To identify crack initiation ( $\sigma_{ci}$ ) and crack damage ( $\sigma_{cd}$ ) thresholds using strain-based analytical methods and evaluate their consistency.**

Crack stress thresholds represent key transition points in brittle rock failure (Martin & Chandler, 1994; Cai et al., 2004). However, their identification remains method-dependent and sometimes inconsistent (Nicksiar & Martin, 2012; Diederichs, 2003). This objective seeks to apply and compare volumetric strain, crack volumetric strain, and Poisson's ratio-based approaches to establish a consistent and physically interpretable identification framework.

### Objective 3

**To develop predictive models for crack stress thresholds ( $\sigma_{ci}$  and  $\sigma_{cd}$ ) using statistical and hybrid machine learning techniques.**

Recent advances demonstrate the capability of artificial neural networks and hybrid optimization methods in predicting mechanical rock properties (Sonmez et al., 2006; Armaghani et al., 2016a). Nevertheless, applications to crack stress thresholds remain limited and often lack optimization-based enhancement. This objective aims to develop and compare multiple linear regression (MLR), nonlinear regression, ANN, DT and hybrid GA- and PSO-based models to improve predictive performance while maintaining physical interpretability.

### Objective 4

**To investigate the residual strength behavior of intact granite under varying confining pressures and assess brittle-ductile transition mechanisms.**

Residual strength plays a crucial role in deep underground engineering but remains less systematically characterized than peak strength (Hobbs, 1966; Cai et al., 2007). Increasing confinement modifies fracture propagation and promotes ductile behavior (Peng & Cai, 2019). This objective aims to evaluate residual strength evolution using multi-failure-state (MFS) triaxial testing and compare the performance of existing residual strength models.

## Objective 5

**To evaluate the applicability of machine learning techniques for predicting uniaxial compressive strength (UCS) and Young's modulus (E) based on index and measurable parameters.**

Predictive modeling of UCS and elastic modulus has become increasingly important for reducing destructive testing and improving design efficiency (Armaghani et al., 2016a; Khatti & Grover, 2023). This objective focuses on assessing MLR, MNLR, ANN and ANFIS for reliable estimation of these parameters within a physics-informed framework.

### 2.2 Conceptual Integration

The final objective of the research is not isolated modeling but integration. The study seeks to connect:

- Stress-dependent stiffness evolution,
- Crack stress threshold identification,
- Confinement-controlled residual behavior, and
- Hybrid machine learning prediction

into a unified interpretation of brittle rock failure.

By combining experimental fracture mechanics principles with optimized data-driven modeling, the research aims to advance intact rock failure characterization beyond traditional peak strength approaches and toward a comprehensive stress-dependent framework.

## 3. MATERIALS AND METHODS

### 3.1 Study Area and Rock Material

The granitic rock samples investigated in this research were collected from the Bábaapáti region, South-West Hungary, a site of significant geotechnical interest due to its use in underground construction and nuclear waste repository studies. The area is dominated by the Carboniferous Mórággy Granite Formation, characterized by megacryst-bearing, medium-grained biotite monzogranites and quartz monzonites (Narimani & Vásárhelyi, 2025).

The selected granite was chosen for its:

- High uniaxial compressive strength (UCS)
- Low porosity and isotropic texture
- Brittle mechanical behavior suitable for crack evolution studies

Specimens were cored to a height-to-diameter (L/D) ratio of 2:1 (50 mm diameter, 100 mm length), with end surfaces ground flat within 0.02 mm tolerance to ensure uniform axial loading (ISRM, 1983).

### 3.2 Experimental Program

A systematic experimental program was designed to address the research objectives. Four distinct datasets were generated or compiled (Table 3-1).

Table 3-1 All dataset analysed in this thesis

Dataset	Purpose	No. of Samples	Reference
UCS for stress-dependent $\nu$	Elastic parameter evolution	42	Narimani et al., 2023b; 2025d
UCS & E prediction	Machine learning models	221	Narimani & Vásárhelyi, 2025
Multiple Failure State (MFS) triaxial	Residual strength & confinement effect	38	Narimani et al., 2025a
Crack stress thresholds	$\sigma_{ci}$ and $\sigma_{cd}$ modeling using hybrid ML	107	Narimani & Vásárhelyi, 2026b

Key experimental considerations:

- All tests were performed according to ISRM guidelines (1983).
- Axial and lateral deformations were measured using strain gauges or LVDTs.
- Loading was applied under quasi-static, displacement-controlled conditions (0.6 kN/s for UCS).

### 3.3 Uniaxial Compression Tests (UCS)

UCS testing provided the baseline mechanical behavior and allowed the assessment of elastic parameters. Each specimen was instrumented to record:

- Axial strain
- Lateral strain

These measurements enabled calculation of:

- Young's modulus (E) – secant, tangent, and average
- Shear modulus (G) – secant, tangent, and average
- Bulk modulus (K) – secant, tangent, and average
- Poisson's ratio ( $\nu$ ) – secant, tangent, and average

Stress-dependent evolution of  $\nu$ , E, G and K was analysed to identify deviations from classical constant-elasticity assumptions (Narimani et al., 2023b; Narimani et al., 2025d; Narimani & Vásárhelyi, 2026a; Gercek, 2007).

### 3.4 Multiple Failure State Triaxial Compression Tests

Triaxial tests were conducted to investigate:

- Failure envelopes under varying confining pressures
- Residual strength evolution
- Brittle–ductile transition

The Multiple Failure State (MFS) approach was applied to 38 samples, where specimens were loaded to failure multiple times under incrementally increasing confining pressures ( $\sigma_3$ ). This allowed extraction of:

- Peak strength ( $\sigma_c$ )
- Residual strength parameters (GSI<sub>r</sub>, RSI, mb,  $\lambda$ )

- Hoek–Brown constant ( $m_i$ ) for intact rock

Residual strength was evaluated using three complementary approaches:

1. **GSI-based model** (Cai et al., 2007): empirical link to rock mass structure
2. **RSI approach** (Walton et al., 2019; 2021): confinement-dependent continuous function
3. **Cohesion-loss model** (Peng & Cai, 2019): mechanism-driven framework separating frictional and cohesive contributions

### 3.5 Machine Learning and Hybrid Optimization

To predict mechanical properties and crack stress thresholds from measurable rock parameters, multiple predictive models were developed (Table 3-2).

Table 3-2 All predictive models used in this thesis

Method	Purpose
Multivariate Linear Regression (MLR)	Benchmark linear correlation
Multivariate Nonlinear Regression (MNLR)	Capture nonlinear relationships
Artificial Neural Networks (ANN)	Predict UCS, E, $\sigma_{ci}$ , $\sigma_{cd}$
Adaptive Neuro-Fuzzy Inference System (ANFIS)	Improve interpretability and generalization
Decision Tree (DT)	Feature importance analysis
Hybrid GA-ANN, PSO-ANN, GA-DT, PSO-DT	Optimize prediction performance

Which input parameters included: UCS, Young’s modulus (E), Poisson’s ratio ( $\nu$ ), P-wave velocity ( $V_p$ ), Porosity, density, Brazilian Tensile Strength (BTS) and shear strength. Moreover, the outputs are: Predicted  $\sigma_{ci}$ ,  $\sigma_{cd}$ , UCS, E.

Also, performance metrics included: Coefficient of determination ( $R^2$ ), Root-mean-square error (RMSE), Mean absolute error (MAE), Variance accounted for (VAF) and a20-index.

The combination of experimental data with hybrid optimization enhanced prediction accuracy while maintaining physical relevance (Narimani & Vásárhelyi, 2025; 2026b).

### 3.6 Data Analysis and Integration

All datasets were analysed to extract:

- Stress-dependent elastic parameters
- Crack stress thresholds
- Residual strength envelopes under confinement

Statistical and ML-based analyses were integrated to provide a unified interpretation of rock failure mechanisms. Key insights from stress–strain curves, volumetric deformation, and hybrid ML predictions were combined to support the **New Scientific Results (NSR)** presented in Section 4.

## 4. New Scientific Results (NSR)

### 4.1 NEW SCIENTIFIC RESULT (1)

#### Stress-Dependent Evolution of Poisson’s Ratio in Intact Different Lithologies

This research demonstrates that Poisson’s ratio ( $\nu$ ) exhibits systematic stress-dependent evolution in five different intact lithologies, and that this evolution follows a consistent

nonlinear trend controlled by progressive microcrack development. The study proves that assuming constant  $\nu$  leads to underestimation of lateral deformation and misinterpretation of crack stress thresholds.

A novel approach was employed to examine the evolution of Poisson ratio values throughout the entire process, spanning from crack initiation to the ultimate failure phase within the UCS test. A newly proposed model was intricately aligned with the experimental data through the application of Equation 4-1 and 4-2.

$$\nu = \nu_0 + \tan(\text{degree})/B \quad \text{Equation 4-1}$$

$$\nu = A + \tan(160\sigma/\sigma_c - 80)/B \quad \text{Equation 4-2}$$

The empirical model developed for the Mórágý granite provides a powerful framework for describing the stress-dependent evolution of Poisson's ratio. To demonstrate its generality and robust predictive capability, I extended its application to four other mechanically significant rock types: Limestone, Marl, Sandstone, and Saltstone (Rock Salt). The computed variations of Poisson's ratio under three conventional definitions, secant, average, and tangent, for all five lithologies indicated in Fig. 4-.

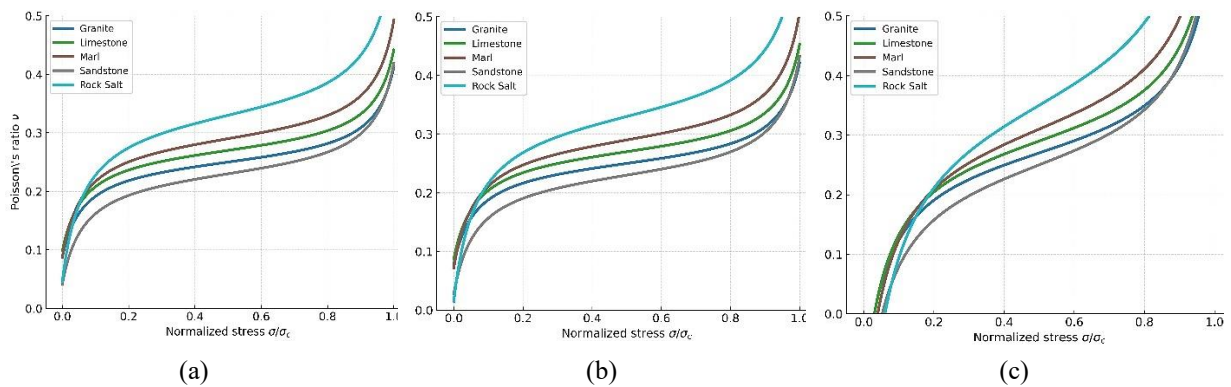


Fig. 4-1 Comparison of the (a) secant, (b) average, and (c) tangent Poisson's ratio ( $\nu$ ) evolutions for five representative lithologies (Granite, Limestone, Marl, Sandstone, and Rock Salt) as a function of normalized stress ( $\sigma/\sigma_c$ ) (Narimani & Vásárhelyi, 2026a).

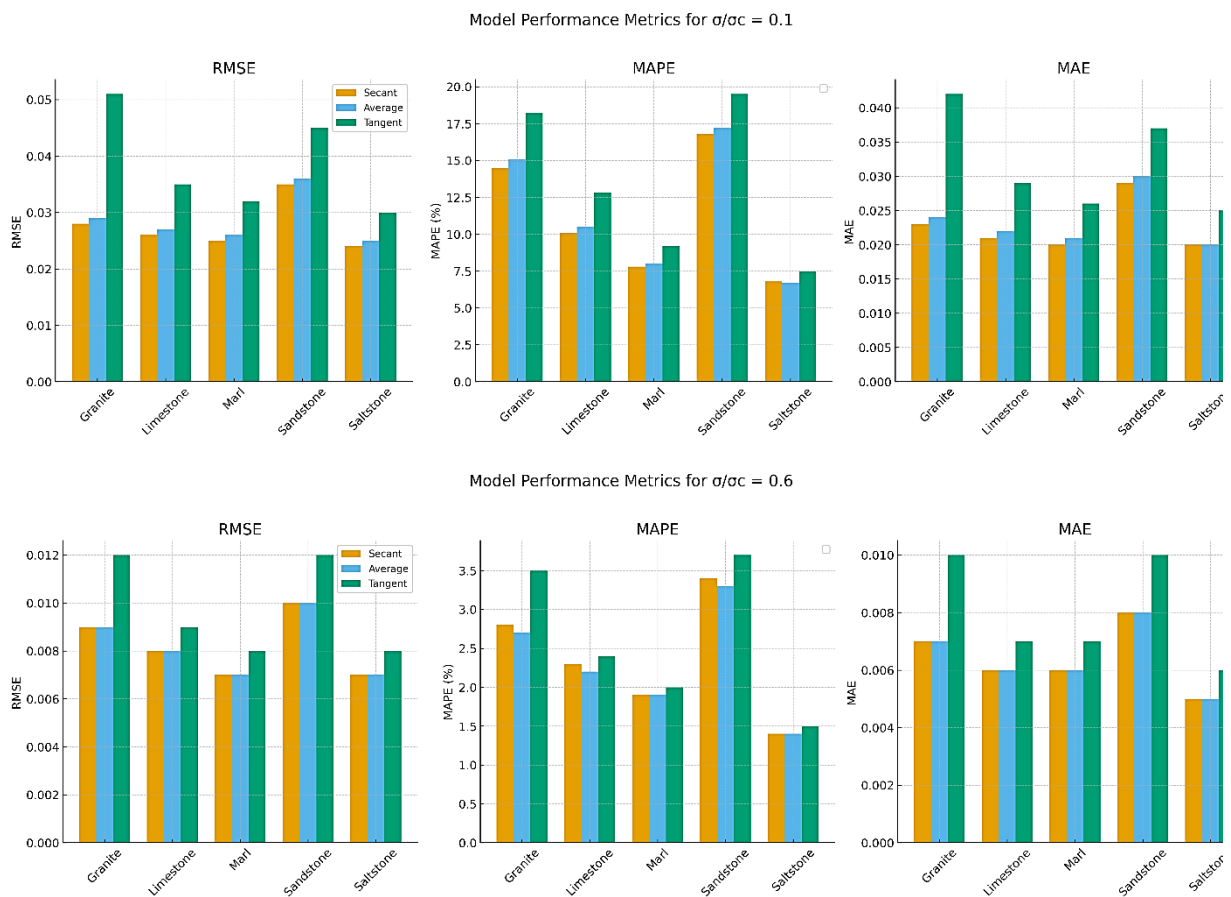
The secant  $\nu$  displays a moderate, continuous increase with stress, representing the overall deformation history. The average  $\nu$  provides an intermediate response with slightly smoother curvature, while the tangent  $\nu$  exhibits a steeper rise, reflecting the local sensitivity of lateral strain to incremental stress. Among the tested lithologies, brittle rocks such as granite and sandstone show more pronounced tangent increases, indicating abrupt volumetric dilation near the crack-damage threshold. Conversely, more ductile materials, such as marl and rock salt, show gentler slopes, consistent with progressive yielding. Together, these trends validate the flexibility of the proposed  $\nu(\sigma/\sigma_c)$  model in describing deformation mechanisms across contrasting lithologies. This extends previous isolated observations (Walsh, 1965; Gercek, 2007) into a multi-lithology validated framework.

For instance, the dynamic fluctuations in Poisson's ratio concerning  $\sigma/\sigma_c$ , encompassing secant, average, and tangent scenarios for 42 granitic samples indicated in Table 4-1.

Table 4-1 Equations and related constants for Poisson's ratio in different cases for granite

Poisson's ratio	Equation	Constant A	Constant B
Secant	$v_{sec} = A_{sec} + \tan(160\sigma/\sigma_c - 80)/B_{sec}$	0.21 - 0.30	25 - 40
Average	$v_{ave} = A_{av} + \tan(160\sigma/\sigma_c - 80)/B_{av3}$	0.22 - 0.31	22 - 40
Tangent	$v_{tan} = A_{tan} + \tan(160\sigma/\sigma_c - 80)/B_{tan}$	0.22 - 0.34	9 - 20

Grouped bar charts of three key statistical indicators, RMSE, MAE, and MAPE, which collectively quantify the predictive accuracy of the developed model, illustrated in Fig. 4-1. According to this figure, the Secant and Average Poisson's ratio formulations yield the most stable and accurate results throughout the loading process. The Tangent Poisson's ratio captures more detailed local variations but is inherently more sensitive to experimental noise. The model performs exceptionally well for more ductile rocks (Marl, Saltstone) and slightly less accurately for brittle rocks (Granite, Sandstone), aligning with their mechanical heterogeneity.



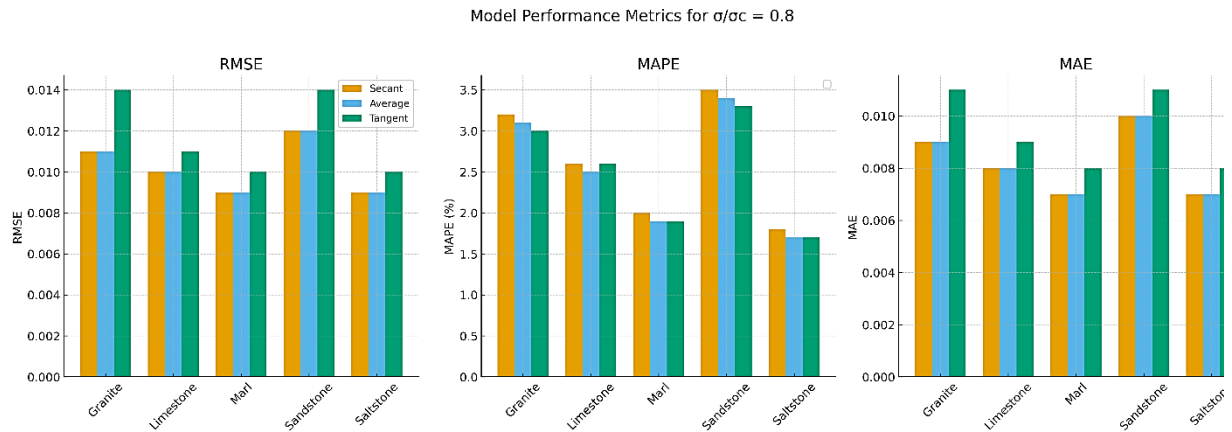


Fig. 4-1 Model performance for five rock types under Secant, Average, and Tangent scenarios at  $\sigma/\sigma_c = 0.1$ ,  $0.6$ , and  $0.8$ , highlighting consistent predictive accuracy across stress levels (Narimani & Vásárhelyi, 2026a).

Engineering implications for this finding are:

- Improves deformation modeling in numerical simulations.
- Refines brittle damage detection.
- Enhances stiffness calibration in deep excavation design.

Related publications:

Narimani, S., Kovács L., Vásárhelyi, B. (2025d): An innovative method to determine the stress-dependency of Poisson's ratio of granitic rocks. *Scientific Reports*, 15, 16111 <https://doi.org/10.1038/s41598-024-75892-2>

Narimani, S., Vásárhelyi, B. (2026a): New Insights into Poisson's Ratio Variability in Rocks Under Load. *International Journal for Numerical and Analytical Methods in Geomechanics*, 50(2), 854-869 <https://doi.org/10.1002/nag.70146>

## 4.2 NEW SCIENTIFIC RESULT (2)

### Stress-Dependent Stiffness Degradation and Elastic Parameter Modeling

The thesis establishes that Young's modulus ( $E$ ), Shear modulus ( $G$ ) and Bulk modulus ( $K$ ) degrade progressively and nonlinearly with increasing stress, and proposes a coupled elastic parameter modeling approach for representing stiffness degradation prior to peak strength.

In this study, extensive UCS tests were conducted on granitic rocks sourced from the Bataapáti site in Hungary. The analysis focused on quantifying how elastic stiffness parameters,  $E$ ,  $G$ , and  $K$  vary from the crack closure phase to ultimate failure. The results showed that all parameters exhibited stress dependency when normalized against the peak uniaxial strength,  $\sigma/\sigma_c$ .

Three distinct definitions— secant, average, and tangent— were applied to evaluate the variation of  $E$  and  $G$ . The relationship between these moduli and the normalized stress was well described using parabolic (quadratic) functions (Equation 4-):

$$E = ax^2 + bx + c \quad \text{Equation 4-3}$$

and

$$G = dx^2 + ex + f$$

For example, the tangent Young's modulus showed a notable decline beyond 60% of the peak strength, reflecting damage accumulation and microcrack coalescence. The secant and average modulus values remained relatively stable until the onset of macro-cracking. The constants for these equations are detailed in Table 4- (E),

Table 4- (G) and Fig. 4-

Table 4-2 Equations and related constants for the *Young's modulus* in different cases.

Young's Modulus	Equation	Constant a	Constant b	Constant c
Secant	$E_{\text{sec}} = ax^2 + bx + c$	-10 to -19	9 to 19	65 to 75
Average	$E_{\text{ave}} = ax^2 + bx + c$	-14 to -24	9 to 18	61 to 76
Tangent	$E_{\text{tan}} = ax^2 + bx + c$	-22 to -67	18 to 36	59 to 77

Table 4-3 Equations and related constants for the *shear modulus* in different cases.

Shear Modulus	Equation	Constant d	Constant e	Constant f
Secant	$G_{\text{sec}} = dx^2 + ex + f$	-5 to -15	3 to 14	21 to 30
Average	$G_{\text{av}} = dx^2 + ex + f$	-4 to -14	2 to 13	25 to 32
Tangent	$G_{\text{tan}} = dx^2 + ex + f$	-20 to -45	8 to 30	22 to 31

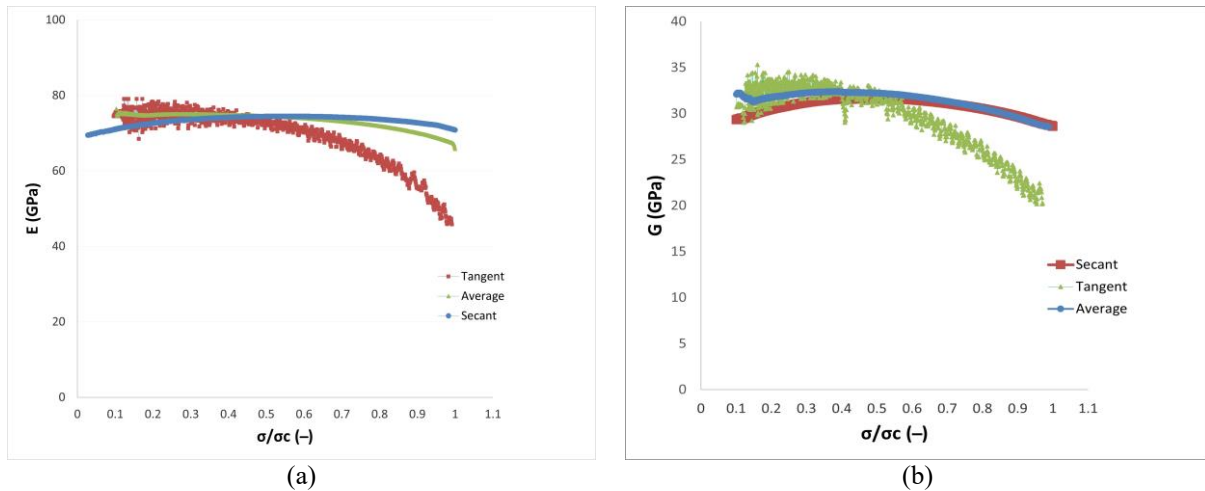


Fig. 4-3 A typical secant, tangent, and average (a) Young's modulus-  $\sigma/\sigma_c$  and (b) shear modulus- $\sigma/\sigma_c$  curves for granitic specimens (Narimani et al., 2023b)

The bulk modulus (K) behaved differently, following a nonlinear increasing trend throughout loading. A novel tangent-based model was proposed:

$$K = C + \frac{3A \cdot \tan(160\sigma/\sigma_c - 80)}{D} \quad \text{Equation 4-4}$$

This formulation produced excellent agreement with experimental values, particularly between the crack closure and crack damage stages. The tangent bulk modulus showed a steeper increase, while secant and average bulk moduli increased almost linearly with stress,

indicating increasing compressibility resistance as microcracks close. The constants for these equations are detailed in Table 4- and Fig. 4-.

Table 4-4 Equations and related constants for the **bulk modulus** in different cases.

Bulk Modulus	Equation	Constant C	Constant D
Secant	$K_{sec} = C + (3C) \tan(160\sigma/\sigma_c - 80)/D$	36 to 55	20 to 40
Average	$K_{av} = C + (3C) \tan(160\sigma/\sigma_c - 80)/D$	41 to 62	20 to 40
Tangent	$K_{tan} = C + (3C) \tan(160\sigma/\sigma_c - 80)/D$	40 to 55	10 to 20

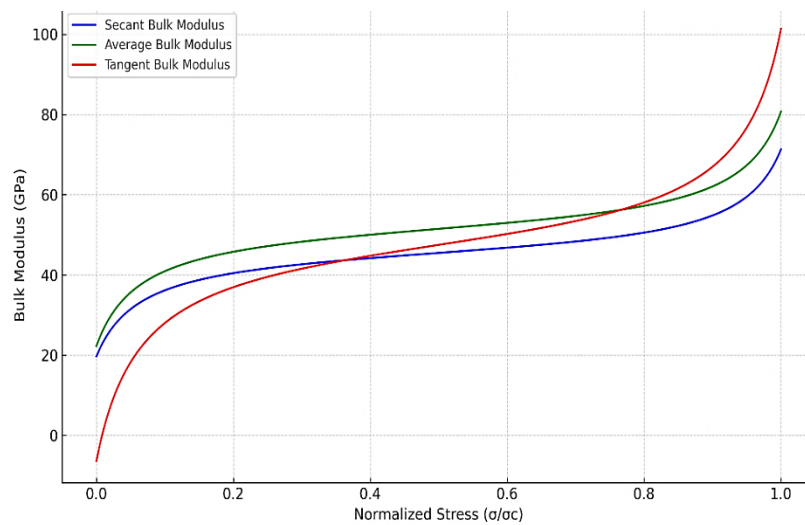


Fig. 4-4 Stress-dependent bulk modulus variations in secant, average, and tangent forms (Narimani et al., 2023b)

Engineering implications for this finding are:

- Improves prediction of tunnel convergence.
- Enables more accurate constitutive modeling before peak failure.
- Supports brittle–ductile transition interpretation.

Related publications:

Narimani S., Davarpanah SM., Kovacs L., Vásárhelyi B. (2023a): Characterization of Poisson’s ratio and Elastic Modulus of granitic rocks: from micro-crack initiation to failure, *15th ISRM Congress 2023 & 72nd Geomechanics Colloquium*, Salzburg, Austria.

Narimani, S., Davarpanah, SM., Kovács L., Vásárhelyi, B. (2023b): Variation of Elastic Stiffness Parameters of Granitic Rock during Loading in Uniaxial Compressive Test. *Applied Mechanics*, 4(2), 445-459 <https://doi.org/10.3390/applmech4020025>

### 4.3 NEW SCIENTIFIC RESULT (3)

#### Machine Learning-Based Prediction of UCS and Young’s Modulus

This research establishes a robust machine learning–based framework for predicting Uniaxial Compressive Strength (UCS) and Young’s modulus (E) of intact rocks using measurable physical and index properties. The developed Artificial Neural Network (ANN) and Adaptive Neuro-Fuzzy Inference System (ANFIS) models demonstrate significantly improved predictive performance compared to conventional regression approaches, while maintaining physical interpretability of input parameters.

Accurate determination of UCS and Young’s modulus is fundamental in rock engineering design, influencing tunnel stability assessment, slope analysis, excavation sequencing, and constitutive model calibration (Hoek & Brown, 1997; Labuz & Zang, 2012). However, laboratory testing for these parameters is: time-consuming, cost-intensive, destructive in nature and often limited by sample availability.

Classical empirical and regression-based approaches provide approximate estimations but frequently fail to capture nonlinear interactions among rock properties. In heterogeneous geological materials, mechanical behavior is governed by complex interdependencies between density, porosity, wave velocity, mineral composition, and microstructure. Therefore, an intelligent modeling approach capable of learning nonlinear multivariate relationships is required.

A comprehensive database comprising 221 rock samples was compiled, including measured values of: density, porosity, P-wave velocity, Brazilian tensile strength and shear strength.

Two primary machine learning approaches were developed:

1. Artificial Neural Networks (ANN)
2. Adaptive Neuro-Fuzzy Inference System (ANFIS)

These were benchmarked against:

- Multivariate Linear Regression (MLR)
- Multivariate Nonlinear Regression (MNLR)

The dataset was divided into training and testing subsets to ensure model generalization and prevent overfitting. Model performance was evaluated as well.

The ANFIS model demonstrated strong performance, particularly in capturing nonlinear transitions between low- and high-strength samples, as shown in Table 4-5 and Table 4-6 for UCS and E respectively. Moreover, sensitivity analysis identified BTS and  $V_p$  as the most critical input variables for predicting UCS and E. Therefore, this confirms that the developed models are not purely statistical black-box systems but remain grounded in physically meaningful rock properties.

*Table 4-5 Performance comparison of UCS for all the models in the training and testing phases.*

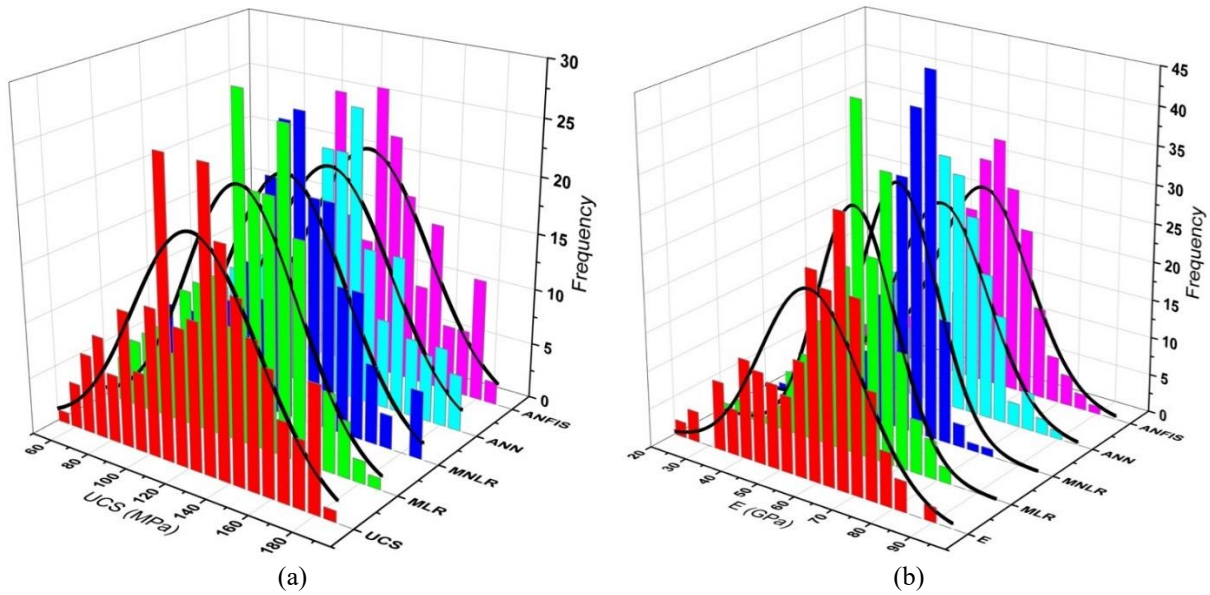
Model	R <sup>2</sup>	Score	RSME	Score	MAE	Score	MAPE	Score	Score	Score	a20-index	Score	Rank
	Training testing		Training testing		Training testing		Training testing		Training testing		Training testing		
MLR	0.74	1	14.606	1	11.908	1	0.101	1	72.64	1	0.91	1	6
	0.80	1	11.612	1	9.192	1	0.080	1	82.95	1	0.95	1	6
MNLR	0.80	2	13.390	2	10.993	2	0.094	2	77.02	2	0.94	2	12
	0.86	2	9.888	2	7.747	2	0.067	2	86.77	2	0.98	2	12
ANN	0.97	3	5.189	3	3.598	3	0.031	3	97.28	3	1	3	18
	0.95	3	6.521	3	4.936	3	0.045	3	95.41	3	1	3	18

ANFIS	0.99	4	2.446	4	1.489	4	0.013	4	99.16	4	1	3	23
	0.97	4	5.544	4	3.502	4	0.031	4	96.43	4	1	3	23

Table 4-6 Performance comparison of E for all the models in the training and testing phases.

Model	R <sup>2</sup>	Score	RSME	Score	MAE	Score	MAPE	Score	VAF (%)	Score	a20-index	Score	Rank
	Training testing		Training testing		Training testing		Training testing		Training testing		Training testing		
MLR	0.72	1	7.555	1	6.250	1	0.119	1	71.17	1	0.86	1	6
	0.62	1	7.523	1	6.171	1	0.100	1	61.58	1	0.89	1	6
MNLR	0.77	2	7.163	2	5.849	2	0.112	2	74	2	0.88	2	12
	0.72	2	6.491	2	5.387	2	0.089	2	70.12	2	0.91	2	12
ANN	0.90	3	4.409	3	3.559	3	0.066	3	90.14	3	0.96	3	18
	0.89	3	3.756	3	2.943	3	0.051	3	88.05	3	0.95	3	18
ANFIS	0.93	4	3.914	4	2.910	4	0.052	4	92.23	4	0.98	4	24
	0.92	4	3.195	4	2.613	4	0.044	4	92.22	4	1	4	24

In addition, the predicted outcomes of the employed models, alongside the respective measured data across all datasets and the prediction errors, are displayed in Fig. 4- for UCS and E. The histogram in the figure illustrates the distribution of errors for normalized data. The concentration of errors around zero indicates the effective performance of the ANFIS model within the designed network for both the UCS and E applications.



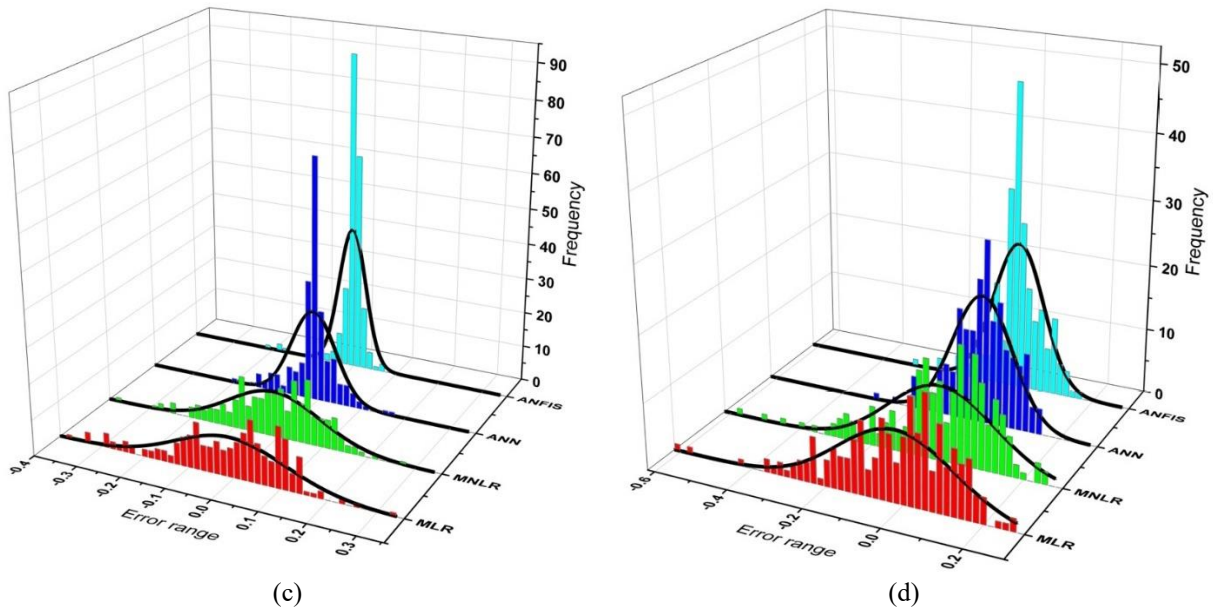


Fig. 4-5 Outputs of all models with the observed data, (a) UCS and (b) E. The change of relative error between actual value and predictive value along with the histogram of errors, (c) UCS and (d) E (Narimani & Vásárhelyi, 2025).

The novelty of this work lies in:

- Integrating a large, experimentally validated dataset with intelligent algorithms
- Providing comparative evaluation between statistical and ML methods within the same framework
- Identifying parameter influence ranking through sensitivity analysis

Unlike many previous studies that focused on single-property prediction, this research presents a unified modeling approach for both strength and stiffness parameters.

Engineering implications for this finding are:

- Rapid estimation of UCS and E during preliminary site investigation
- Reduced dependence on destructive laboratory testing
- Improved parameter input for numerical modeling
- Practical applicability in data-scarce conditions

In engineering practice, such predictive capability enables more efficient decision-making during early design stages while maintaining acceptable accuracy.

Related publications:

Narimani, S., Vásárhelyi, B. (2025): Leveraging machine learning for precision prediction of geomechanical properties of granitic rocks: a comparative analysis of MLR, ANN, and ANFIS models. *Earth Science Informatics*, 18(1), 91 <https://doi.org/10.1007/s12145-024-01653-4>

#### 4.4 NEW SCIENTIFIC RESULT (4)

##### Intelligent Algorithm–Based Estimation of Crack Stress Thresholds in Granitic Rocks

This research introduces a hybrid intelligent modeling framework for accurately estimating crack initiation ( $\sigma_{ci}$ ) and crack damage ( $\sigma_{cd}$ ) thresholds in granitic rocks using measurable mechanical and physical properties. Unlike conventional analytical or empirical methods that rely solely on strain or acoustic emission analysis, this approach integrates optimized machine learning (ML) algorithms with physically grounded fracture mechanics principles to establish reliable and generalizable prediction models.

Crack stress thresholds,  $\sigma_{ci}$  and  $\sigma_{cd}$ , mark critical transitions in the mechanical response of brittle rocks, separating stable microcrack propagation from unstable macrofracturing. Accurate identification of these thresholds is fundamental for assessing the onset of damage, energy dissipation, and stiffness degradation in underground structures and deep rock engineering. However, experimental determination of  $\sigma_{ci}$  and  $\sigma_{cd}$  through strain-based or acoustic methods is often time-consuming, sensitive to experimental noise, and limited by instrumentation resolution (Martin & Chandler, 1994; Nicksiar & Martin, 2012).

Given the nonlinear relationships among physical, mechanical, and fracture parameters, intelligent algorithms such as Artificial Neural Networks (ANN), Decision Trees (DT), and hybrid optimization techniques (GA-ANN, PSO-ANN) provided a powerful alternative to traditional models. This study thus develops a data-driven predictive system capable of estimating  $\sigma_{ci}$  and  $\sigma_{cd}$  directly from measurable rock properties, reducing the dependence on extensive laboratory testing.

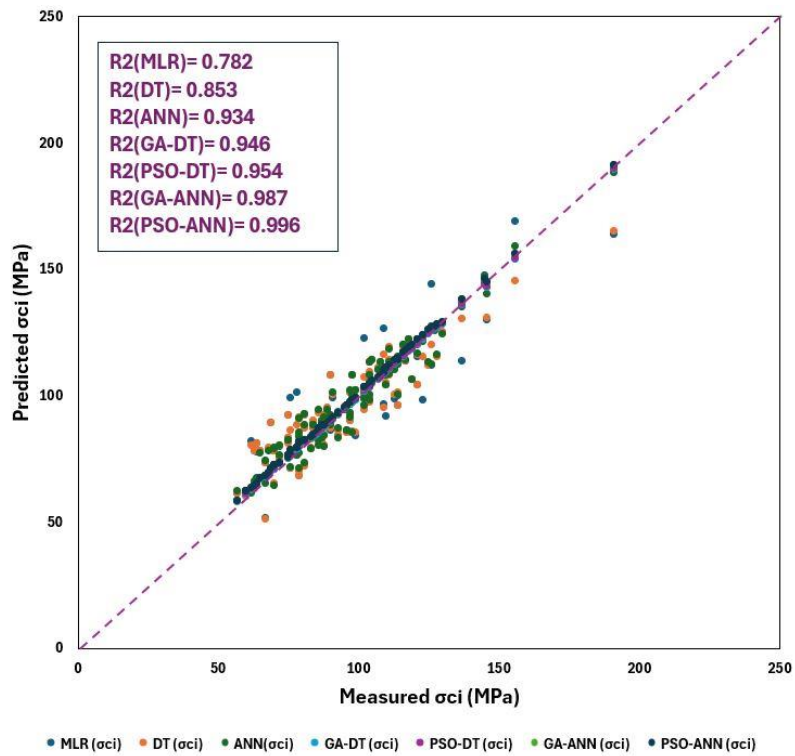
A dedicated dataset of 107 granitic samples from was compiled from extensive laboratory testing. Each sample contained the following input: UCS, E and  $\nu$ . The corresponding outputs were the experimentally derived crack thresholds,  $\sigma_{ci}$  and  $\sigma_{cd}$  determined through strain-based and volumetric strain approaches. These parameters were selected based on their established influence on crack development and deformation behavior. The input parameters and output variables used for intelligent estimation of crack stress thresholds are summarized in Table 4-7.

*Table 4-7 Sensitivity Rankings and Practical Recommendations (Narimani & Vásárhelyi, 2026b).*

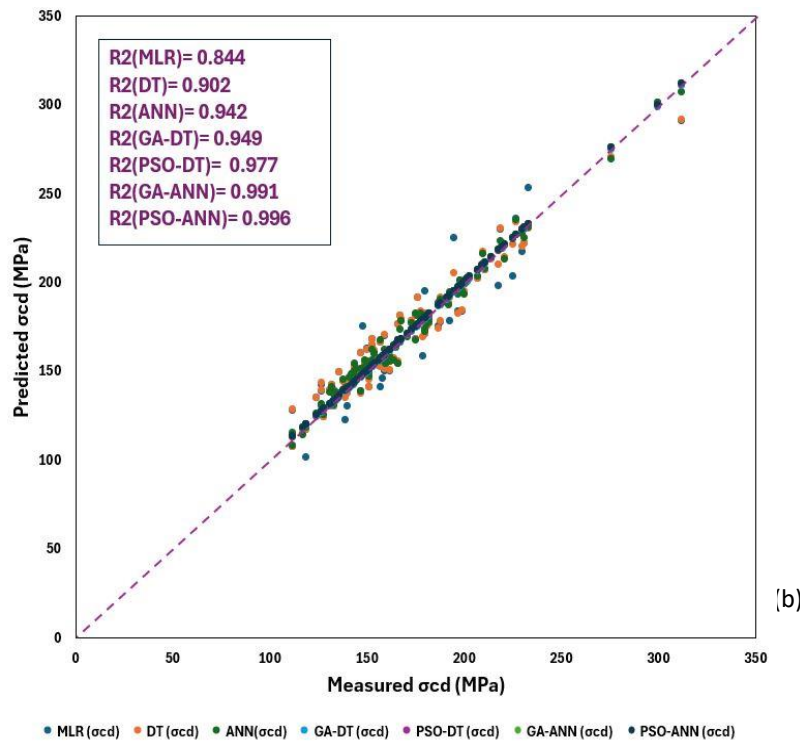
<b>Input Parameter</b>	<b>Sensitivity for <math>\sigma_{ci}</math></b>	<b>Sensitivity for <math>\sigma_{cd}</math></b>	<b>Engineering Importance</b>
UCS	0.98853 (Highest)	0.97462 (Highest)	Essential; primary focus in data collection
E (Young's Modulus)	0.86542	0.98068	Important; highly recommended for precision measurements
$\nu$ (Poisson's Ratio)	0.42318	0.37764	Lower priority; useful for supplementary analysis

The intelligent models demonstrated a strong capability in estimating both crack initiation and crack damage stress thresholds across the investigated range of mechanical conditions. Predicted values showed good agreement with experimentally determined thresholds, indicating that the models effectively captured the underlying relationships between mechanical parameters and crack stress behavior (Fig. 4-6). These figures provide a detailed

visualization of how well each model replicates the experimentally measured stress values and highlight the clear progression of performance improvement from conventional statistical models to machine learning techniques and finally to hybrid optimization frameworks.



(a)



(b)

Fig. 4-6 Measured and predicted (a)  $\sigma_{ci}$  and (b)  $\sigma_{cd}$  using different models for all samples (Narimani & Vásárhelyi, 2026b).

Model performance was evaluated using standard statistical indicators, including the coefficient of determination and error-based metrics. The results indicate that the intelligent algorithms provide stable and reliable estimates of crack stress thresholds within the investigated parameter space. Differences in estimation accuracy among the applied models reflect variations in their ability to represent nonlinear interactions between input variables (Table 4-8 and Table 4-9).

Table 4-8 Performance comparison of  $\sigma_{ci}$  for all the models.

Model	R <sup>2</sup>	Score	RMSE	Score	MAE	Score	MAPE	Score	VAF (%)	Score	Rank
MLR	0.782	1	10.660	1	8.540	1	0.093	1	78.72	1	5
DT	0.853	2	9.002	2	7.346	2	0.082	2	84.84	2	10
ANN	0.934	3	5.965	3	4.790	3	0.053	3	93.34	3	15
GA-DT	0.946	4	3.819	4	2.628	4	0.022	4	94.69	4	20
PSO-DT	0.954	5	2.753	5	1.573	5	0.017	5	95.42	5	25
GA-ANN	0.987	6	2.113	6	1.104	6	0.009	6	99.06	6	30
PSO-ANN	0.996	7	1.065	7	0.508	7	0.005	7	99.68	7	35

Table 4-9 Performance comparison of  $\sigma_{cd}$  for all the models.

Model	R <sup>2</sup>	Score	RMSE	Score	MAE	Score	MAPE	Score	VAF (%)	Score	Rank
MLR	0.844	1	10.129	1	8.078	1	0.049	1	82.45	1	5
DT	0.902	2	7.813	2	6.388	2	0.039	2	89.52	2	10
ANN	0.942	3	4.676	3	3.785	3	0.023	3	92.40	3	15
GA-DT	0.949	4	3.101	4	2.812	4	0.020	4	95.66	4	20
PSO-DT	0.977	5	1.671	5	1.231	5	0.014	5	97.85	5	25
GA-ANN	0.991	6	1.102	6	0.85	6	0.008	6	99.11	6	30
PSO-ANN	0.996	7	0.522	7	0.446	7	0.003	7	99.83	7	35

In order to provide an integrated comparison of model performance, a Taylor diagram was employed to simultaneously evaluate the correlation and standard deviation of the machine learning algorithms. This representation enables a concise assessment of the relative agreement between predicted and experimentally determined crack stress thresholds (Fig. 4-7).

This study represents the first hybrid GA/PSO-optimized intelligent framework specifically designed to estimate crack initiation and damage stresses in granitic rocks. It bridges fracture

mechanics fundamentals with data-driven intelligence, offering both predictive accuracy and interpretability. The approach reduces experimental dependency, accelerates parameter estimation, and advances the frontier of intelligent fracture mechanics.

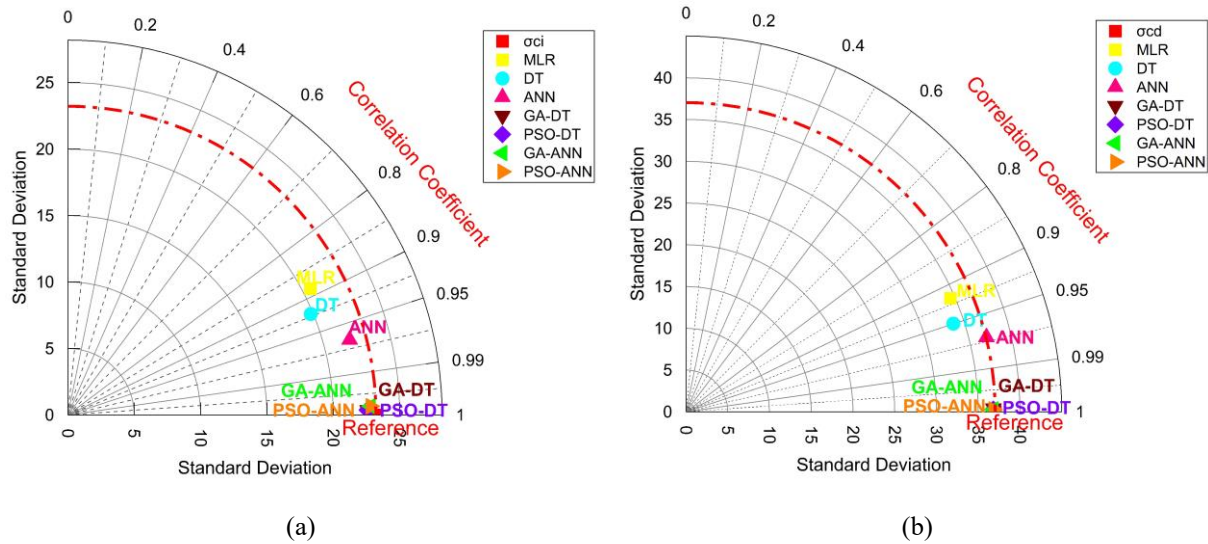


Fig. 4-7 Demonstration of the Taylor diagram for all data based on MLR, DT, ANN, GA-DT, GA-ANN, PSO-DT and PSO-ANN models for (a)  $\sigma_{ci}$  and (b)  $\sigma_{cd}$  (Narimani & Vásárhelyi, 2026b).

Engineering and scientific implications for this finding are:

- Predictive Design Tool: Enables rapid estimation of crack thresholds in design stages without destructive testing.
- Enhanced Failure Modelling: Improves constitutive models by integrating data-driven  $\sigma_{ci}$  and  $\sigma_{cd}$  estimates into stress–strain analyses.
- Optimization Framework: Demonstrates the synergy between experimental rock mechanics and intelligent optimization algorithms.
- Generalization: Provides a transferable methodology for other brittle lithologies beyond granitic formations.

Related publications:

Narimani, S., Vásárhelyi, B. (2026b): Hybrid Machine Learning Models for Predicting Crack Stress Thresholds in Granitic Rocks: An Optimization-Based Approach. *Rock Mechanics & Rock Engineering*, under publication

Narimani S., Davarpanah SM., Vásárhelyi B. (2025b): Predicting the Crack Stress Thresholds of the Intact Granitic Rocks by machine learning and multivariate analysis techniques, *Eurock 2025 – Expanding the Underground Space*, Trondheim, Norway, 16-20 June, ISBN 978-82-8208-079-8.

## 4.5 NEW SCIENTIFIC RESULT (5)

### Interdependency of Confining Pressure and GSI in Residual Strength Determination

This research establishes a quantitative relationship between confining pressure and Geological Strength Index (GSI) in determining the residual strength of intact granitic rocks, introducing a modified confinement-dependent residual strength model that captures the brittle–ductile transition more accurately than classical approaches.

By integrating Multiple Failure State (MFS) triaxial test data with analytical and regression-based modeling, this study demonstrates that residual strength is not solely a function of confining pressure, but evolves in a coupled manner with microstructural degradation reflected through the GSI and the confinement-induced damage parameter  $\lambda$ .

Traditional residual strength models such as the GSI-based formulation (Cai et al., 2007), the cohesion-loss model (Peng & Cai, 2019) and the RSI approach (Walton et al., 2021) have provided useful empirical representations for post-peak behavior in rocks. However, they typically treat GSI as a fixed descriptor of rock mass structure, independent of the confining pressure.

Experimental evidence from the present study, based on systematic triaxial MFS testing of granitic rocks from the Bátaapáti region, reveals that confinement actively modifies the degradation pattern of the rock structure, and therefore the effective GSI evolves with increasing  $\sigma_3$  (minor principal stress).

This finding challenges the conventional assumption of GSI constancy in residual conditions and introduces the concept of a “confinement-responsive GSI” ( $GSI_r$ ) to improve residual strength estimation.

A total of 38 triaxial compression tests were conducted under confining pressures ranging from 5 to 60 MPa, applying the Multiple Failure State (MFS) methodology to obtain both peak ( $\sigma_p$ ) and residual ( $\sigma_r$ ) strength parameters for each specimen.

Three modeling frameworks were evaluated:

- Classical GSI-Based Model (Cai et al., 2007)
- Cohesion-loss model (Peng & Cai, 2019)
- RSI approach (Walton et al., 2019 & 2021)

The following non-linear regression (Equation 4-5) was found plotting the deviator stress in the function of the confining pressure for granitic rocks:

$$\sigma_1 - \sigma_3 = b \sigma_3^c \quad \text{Equation 4-5}$$

Where  $b$  and  $c$  are material constants that reflect the strength characteristics of the rock.

Using cohesion loss model, suggested by Peng & Cai (2019) which reflects how confining pressure influences the post-peak behavior of rocks, providing a more dynamic interpretation of rock strength than conventional static approaches:

$$b \sigma_3^c = (m_b UCS \sigma_3)^{0.5} \quad \text{Equation 4-6}$$

Equation (4-7) to Equation (4-10) expand on this concept by introducing a logarithmic relationship between GSI and confining pressure.

$$GSI = x \ln(\sigma_3) + z \quad \text{Equation 4-7}$$

$$x = 28(2c - 1) \quad \text{Equation 4-8}$$

$$z = 100 + 28*(2\ln(b) - \ln(m_i) - \ln(UCS)) \quad \text{Equation 4-9}$$

$$m_b = \frac{b^2}{UCS} \sigma_3^{2c-1} \quad \text{Equation 4-10}$$

Fig. 4-8 illustrates the dependency of GSI and  $m_b$  on confining stress, directly challenging the Walton et al. (2021) hypothesis, which suggests that GSI remains unaffected by confinement in intact rocks. The graph demonstrates a clear logarithmic trend, reinforcing the notion that GSI decreases at higher confining pressures. This insight underscores the nonlinear-value nature of rock mass strength under varying stress environments, making a compelling case for re-evaluating existing models that treat GSI as a constant-value. Moreover, The integration of  $\sigma_3$ –GSI<sub>r</sub> coupling within the residual strength framework provides a more realistic basis for representing post-peak rock behavior in the Hoek–Brown failure criterion. Specifically, the residual Hoek–Brown parameter  $m_b$  can be expressed as a function of both  $\sigma_3$  and GSI<sub>r</sub>, allowing for adaptive strength estimation under evolving stress and structural conditions (Fig. 4-8b).

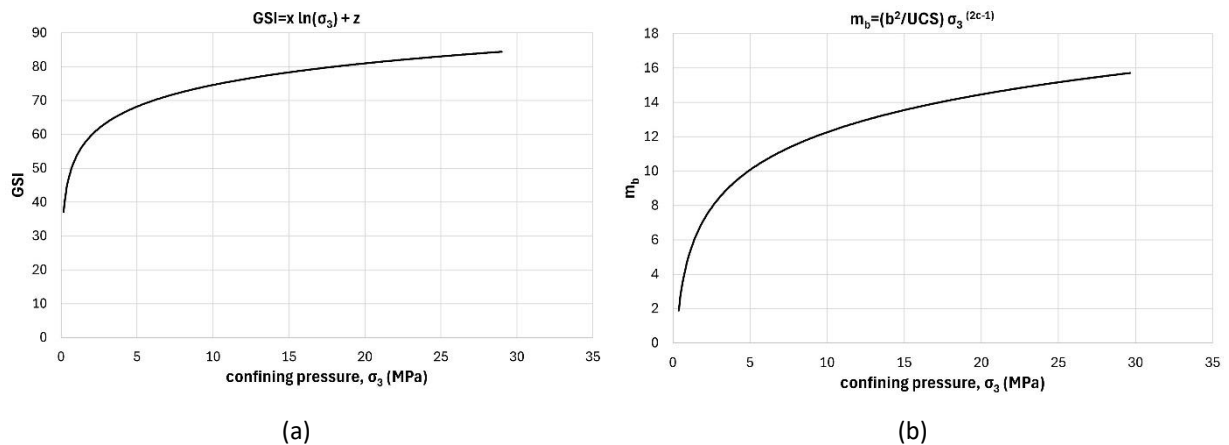


Fig. 4-8 Relationship between (a) GSI<sub>r</sub> and (b)  $m_b$  in function of confining pressure ( $\sigma_3$ ) (Narimani et al., 2025a).

This study is the first to quantify the coupled evolution of GSI and confining pressure for intact granitic rocks within a residual strength context. The proposed confinement–GSI model captures both brittle-ductile transition and post-peak deformation mechanisms within a physically interpretable, empirically validated framework. The finding bridges the gap between empirical GSI formulations and mechanistic strength behavior, providing a new perspective on residual characterization in high-confinement rock mechanics.

Engineering and scientific implications for this thesis are:

- **Enhanced Post-Peak Prediction:** Incorporating confinement-dependent GSI improves residual strength prediction accuracy, critical for deep tunnel and underground cavern design.

- Unified Framework: Bridges rock mass classification (GSI) with triaxial mechanical behavior, enabling integration into numerical modeling.
- Mechanistic Insight: Demonstrates that residual strength evolution is a dual function of confinement-induced plasticity and microstructural degradation.
- Practical Utility: Facilitates reliable input parameters for Hoek–Brown-based models and FLAC3D/PLAXIS constitutive simulations in high-stress conditions.

Related publications:

Narimani, S., Davarpanah, SM., Török, Á, Vásárhelyi, B. (2025a): Residual Strength of Granitic Rocks: Interplay Between GSI and Confining Pressure. *Scientific Reports*, 15, 28986 <https://doi.org/10.1038/s41598-025-14419-9>

## 5 LIST OF PUBLICATIONS

### *Journal papers*

#### *(Publications Related to thesis)*

1. **Narimani, S.**, Davarpanah, SM., Kovács L., Vásárhelyi, B. (2023b): Variation of Elastic Stiffness Parameters of Granitic Rock during Loading in Uniaxial Compressive Test. *Applied Mechanics*, 4(2), 445-459 <https://doi.org/10.3390/applmech4020025>, **Q2**
2. **Narimani, S.**, Davarpanah, SM., Bar, N., Török, Á., Vásárhelyi, B. (2023c): Geological Strength Index Relationships with the Q-System and Q-Slope. *Sustainability*, 15(14), 11233 <https://doi.org/10.3390/su151411233>, **Q1**
3. **Narimani, S.**, Davarpanah, SM., Vásárhelyi, B. (2024): Estimation of the Poisson's Ratio of the Rock Mass. *Periodica Polytechnica Civil Engng*, 68(1), 274-288 <https://doi.org/10.3311/PPci.22689>, **Q2**
4. **Narimani, S.**, Davarpanah, SM., Török, Á, Vásárhelyi, B. (2025a): Residual Strength of Granitic Rocks: Interplay Between GSI and Confining Pressure. *Scientific Reports*, **15**, 28986 <https://doi.org/10.1038/s41598-025-14419-9>, **Q1**
5. **Narimani, S.**, Kovács L., Vásárhelyi, B. (2025d): An innovative method to determine the stress-dependency of Poisson's ratio of granitic rocks. *Scientific Reports*, 15, 16111 <https://doi.org/10.1038/s41598-024-75892-2>, **Q1**
6. **Narimani, S.**, Vásárhelyi, B. (2025): Leveraging machine learning for precision prediction of geomechanical properties of granitic rocks: a comparative analysis of MLR, ANN, and ANFIS models. *Earth Science Informatics*, 18(1), 91 <https://doi.org/10.1007/s12145-024-01653-4>, **Q1**
7. **Narimani, S.**, Vásárhelyi, B. (2026a): New Insights into Poisson's Ratio Variability in Rocks Under Load. *International Journal for Numerical and Analytical Methods in Geomechanics*, 50(2), 854-869 <https://doi.org/10.1002/nag.70146>, **Q1**
8. **Narimani, S.**, Vásárhelyi, B. (2026b): Hybrid Machine Learning Models for Predicting Crack Stress Thresholds in Granitic Rocks: An Optimization-Based Approach. *Rock Mechanics & Rock Engineering*, *accepted, under publication*, **Q1**
9. **Narimani, S.**, Vásárhelyi, B. (2026c): Estimation of the Hoek-Brown constant  $m_i$  from analyzing the uniaxial compressive test. *International Journal of Geo-Engineering*, under review, **Q1**

10. **Narimani, S.**, Davarpanah, SM., Vásárhelyi, B. (2026): Reviewing the concept of Multiple Failure State Triaxial Test in Rock Mechanics. *Rock Mechanics Rock Engineering, under review*, **Q1**

**(Publications not related to thesis)**

1. **Narimani, S.**, Davarpanah, SM., Bar N., Vásárhelyi, B. (2025c): Analyzing Drill Core Logging Using Rock Quality Designation–60 Years’ Experience from Modifications to Applications. *Applied Sciences*, 15(3), 1309 <https://doi.org/10.3390/app15031309>, **Q1**
2. Vásárhelyi, B., **Narimani, S.**, Davarpanah, SM., Mocsár G. (2024): Modeling Brittle-to-Ductile Transitions in Rock Masses: Integrating the Geological Strength Index with the Hoek–Brown Criterion. *Applied Mechanics*, 5, 634-645 <https://doi.org/10.3390/applmech5040036>, **Q2**
3. Davarpanah, SM., **Narimani, S.**, Sharghi M., Vásárhelyi, B. (2025): Introducing Coefficients of Curvature (Cc) and Uniformity (Cu) Based on RQD for Rock Mass Characterization. *Rock Mechanics Letters* 2(1), 76-78 <https://doi.org/10.70425/rml.202501.10>
4. Davarpanah, M., **Narimani, S.**, Sharghi, M., Vásárhelyi, B. Török, Á. (2023a): Brittle-Ductile Transition Stress of Different Rock Types and Its Relationship with Uniaxial Compressive Strength and Hoek-Brown Material Constant. *Scientific Reports*, 13, 1186 <https://doi.org/10.1038/s41598-023-28513-3>, **Q1**
5. Gholipour, M., **Narimani, S.**, Davarpanah, SM., Vásárhelyi, B. (2025): Evaluating Minimum Support Pressure for Tunnel Face Stability: Analytical, Numerical, and Empirical Approaches. *Journal of Experimental and Theoretical Analyses*, 3(1), 2 <https://doi.org/10.3390/jeta3010002>
6. **Narimani S.**, Chakeri H., Davarpanah SM. (2018): Simple and non-linear regression techniques used in sandy-clayey soils to predict the pressuremeter modulus and limit pressure: a case study of Tabriz subway. *Periodica Polytechnica Civil Engng*, 62(3): 825-839. doi: 10.3311/PPci.12063, IF: 1.07, **Q2**
7. Davarpanah, SM., Sharifzadeh, M., Sattarvand, J., **Narimani, S.** (2016) Evaluation of Building Displacement Induced By EPB Tunneling Through GPS-GNSS Monitoring System and Back Analysis Technique (Tabriz Subway Twin Tunnels), *Civil Engineering Journal*, <https://doi.org/10.28991/cej-2016-00000032>, **Q1**
8. **Narimani, S.**, Davarpanah, SM., Sattarvand, J. (2016) Prediction of Hydro-mechanical Stability of Dam: Using Calibrated Model from Back Analysis and Monitoring Data, *Civil Engineering Journal*, <https://doi.org/10.28991/cej-2016-00000044> , **Q1**

**Conference proceedings:**

9. **Narimani S.**, Davarpanah SM., Vásárhelyi B. (2025b): *Predicting the Crack Stress Thresholds of the Intact Granitic Rocks by machine learning and multivariate analysis techniques*, Eurock 2025 – Expanding the Underground Space Trondheim, Norway, 16-20 June, ISBN 978-82-8208-079-8.
10. **Narimani S.**, Kovacs L., Vásárhelyi B. (2024): *A Poisson-tényező, mint feszültségfüggő paraméter alternatív meghatározása*, Mérnökgeológia-Kőzetmechanika 2024, Budapest.
11. Vásárhelyi B., **Narimani S.**, Davarpanah SM., Mocsár G. (2024): *Közzettestek ridegképlékeny átmenetének meghatározása a Geológiai Szilárdsági Index (GSI) és a Hoek-Brown törési határfeltétel ismeret*, Mérnökgeológia-Kőzetmechanika 2024, Budapest.

12. **Narimani S.**, Davarpanah SM., Kovacs L., Vásárhelyi B. (2023a): *Characterization of Poisson's ratio and Elastic Modulus of granitic rocks: from micro-crack initiation to failure*, 15th ISRM Congress 2023 & 72nd Geomechanics Colloquium, Salzburg, Austria.
13. Davarpanah SM., **Narimani S.**, Besharatinezhad A., Khodabandeh M., Török Á., Vásárhelyi B. (2022): *Applicability of the recently proposed semi-empirical failure criterion for different rock types by using triaxial test data*, Fifth symposium of the Macedonian Association for Geotechnics, 2022 Macedonian Association for Geotechnics, ISBN 978-9989-2053-4-7.
14. Besharatinezhad A., Khodabandeh M. **Narimani S.**, Török Á., Davarpanah SM., Vásárhelyi B. (2022): *Analytical and numerical investigation of the critical height of vertical rock slope*, Fifth symposium of the Macedonian Association for Geotechnics, 2022 Macedonian Association for Geotechnics, ISBN 978-9989-2053-4-7.
15. Keivani H., **Narimani S.**, Vásárhelyi B. Davarpanah SM. (2018): Experimental study on hydraulic fracturing of homogenous and non-homogenous rock samples. In: Török Á, Görög P.; Vásárhelyi B. (eds), *Mérnökgeológia-Kőzetmechanika* 201-209.

## REFERENCES

- Armaghani DJ, Mohamad ET, Hajihassani M, Yagiz S & Motaghedi H. (2016a). Application of several non-linear prediction tools for estimating uniaxial compressive strength of granitic rocks and comparison of their performances. *Eng Comput*, 32(2), 189–206.
- Atkinson BK. (2015). *Fracture Mechanics of Rock*. Academic Press, 1st Edition, ISBN: 9781483292748.
- Bieniawski, Z. T. (1967). Mechanism of brittle fracture of rock: Part I—Theory of the fracture process. *International Journal of Rock Mechanics and Mining Sciences*, 4(4), 395–406.
- Brace, W. F., Paulding, B. W., & Scholz, C. (1966). Dilatancy in the fracture of crystalline rocks. *Journal of Geophysical Research*, 71(16), 3939–3953.
- Cai, M. , Kaiser, P. K. , Uno, H. , Tasaka, Y. , & Minami, M. (2004). Estimation of rock mass deformation modulus and strength of jointed hard rock masses using the GSI system. *Int J Rock Mech. Mining Sci.*, 41(1), 3–19.
- Cai, M. , Kaiser, P. K. , Tasaka, Y. , & Minami, M. (2007). Determination of residual strength parameters of jointed rock masses using the GSI system. *Int. J. Rock Mech. Min. Sci.*, 44, 247–265.
- Diederichs, M. S. (2003). Rock fracture and collapse under low confinement conditions. *Rock Mechanics and Rock Engineering*, 36(5), 339–381.
- Gercek, H. (2007). Poisson's ratio values for rocks. *Int. J. Rock Mech. Min. Sci*, 44(1), 1–13.
- Hobbs, D. W. (1966). A study of the behaviour of a broken rock under triaxial compression, and its application to mine roadways. *Int. J. Rock Mech. Min. Sci. Geomech. Abs*, 3, 11–43.
- Hoek E & Brown ET. (1997). Practical estimates of rock mass strength. *Int. J. Rock Mech. Mining Sci. Geomech Abs*, 34(8), 1165–1186.
- ISRM. (1983). Suggested methods for determining the strength of rock materials in triaxial compression: Revised version. *Int. J. Rock Mech. Min. Sci. & Geomech. Abst.* , 20(6), 285–290.
- Jaeger, J. C. (1969). Behavior of closely jointed rock. 11th US Symposium on Rock Mechanics.

- Khatti J & Grover KS. (2023). Estimation of Intact Rock Uniaxial Compressive Strength using Advanced Machine Learning. *Tran Infra Geotech*.
- Kovári, K. & Tisa, A. (1975). Multiple failure state and strain controlled triaxial tests. *Rock Mech*, 7, 17–33.
- Labuz, J. F. , & Zang, A. (2012). Mohr–Coulomb failure criterion. In R. Ulusay (Ed.), *The ISRM Suggested Methods for Rock Characterization, Testing and Monitoring*, 227–231.
- Martin, C. D. & Chandler, N. A. (1994). The progressive fracture of Lac du Bonnet granite. *International Journal of Rock Mechanics and Mining Sciences*, 31(6), 643–659.
- Nicksiar, M. & Martin, C. D. (2012). Crack initiation stress in low-porosity rocks. *Rock Mechanics and Rock Engineering*, 45(4), 607–617.
- Peng, J. & Cai, M. (2019). A cohesion loss model for determining residual strength of intact rocks. *International Journal of Rock Mechanics and Mining Sciences*, 119, 131–139.
- Sonmez H, Gokceoglu C, Nefeslioglu HA & Kayabasi A. (2006). Estimation of rock modulus: for intact rocks with an artificial neural network and for rock masses with a new empirical equation. *Int J Rock Mech Min Sci*, 43(2), 224–235.
- Walsh, J. B. (1965). The effect of cracks on the compressibility of rock. *J. Geophys. Res.*, 70(2), 381–389.
- Walton, G., Labrie, D. & Alejano, L. R. (2019). On the Residual Strength of Rocks and Rock masses. *Rock Mech. Rock Engng.* , 52(11), 4821–4833.
- Walton, G., Gaines, S., & Alejano, L. R. (2021). Validity of continuous-failure-state unloading triaxial tests as a means to estimate the residual strength of rock. *J. Rock Mech. Geotech. Engng.*, 13(4), 717–726.
- Yu Z, Zhou J & Hu L. (2023). Prediction of compressive strength of granite: use of machine learning techniques and intelligent system. *Earth Sci Inf*, 16, 4113–4129.